Solar Phys
DOI 10.1007/s11207-013-0341-5

The 22-Year Hale Cycle in Cosmic Ray Flux – Evidence for Direct Heliospheric Modulation

S.R. Thomas · M.J. Owens · M. Lockwood

Received: 21 May 2012 / Accepted: 29 May 2013

Abstract The ability to predict times of greater galactic cosmic ray (GCR) fluxes is important for reducing the hazards caused by these particles to satellite communications, aviation, or astronauts. The 11-year solar-cycle variation in cosmic rays is highly correlated with the strength of the heliospheric magnetic field. Differences in GCR flux during alternate solar cycles yield a 22-year cycle, known as the Hale Cycle, which is thought to be due to different particle drift patterns when the northern solar pole has predominantly positive (denoted as $qA > 0$ cycle) or negative ($qA < 0$) polarities. This results in the onset of the peak cosmic-ray flux at Earth occurring earlier during $qA > 0$ cycles than for $qA < 0$ cycles, which in turn causes the peak to be more dome-shaped for $qA > 0$ and more sharply peaked for $qA < 0$. In this study, we demonstrate that properties of the large-scale heliospheric magnetic field are different during the declining phase of the $qA < 0$ and $qA > 0$ solar cycles, when the difference in GCR flux is most apparent. This suggests that particle drifts may not be the sole mechanism responsible for the Hale Cycle in GCR flux at Earth. However, we also demonstrate that these polarity-dependent heliospheric differences are evident during the space-age but are much less clear in earlier data: using geomagnetic reconstructions, we show that for the period of 1905 – 1965, alternate polarities do not give as significant a difference during the declining phase of the solar cycle. Thus we suggest that the 22-year cycle in cosmic-ray flux is at least partly the result of direct modulation by the heliospheric magnetic field and that this effect may be primarily limited to the grand solar maximum of the space-age.

Keywords 22-year cycle · Cosmic rays · Heliospheric current sheet · Solar variability · Polarity reversal

1. Introduction

During the recent solar minimum, which was longer and deeper than others observed for over a century (Lockwood, 2010), galactic cosmic-ray (GCR) flux has reached its highest

S.R. Thomas (✉) · M.J. Owens · M. Lockwood
University of Reading, Reading, UK
e-mail: s.r.thomas@pgr.reading.ac.uk

Published online: 24 July 2013

values of the space-age (Mewaldt *et al.*, 2010). The high GCR flux has implications for satellites, spacecraft, and aviation (*e.g.* Hapgood, 2010) due to their high energies, making the ability to predict times of greater fluxes of cosmic rays critical for mission planning and reducing such hazards. It is also important to study the propagation and modulation of GCRs throughout the heliosphere for the purposes of long-term reconstructions of solar parameters (*e.g.* McCracken *et al.*, 2004; Usoskin, Bazilevskaya, and Kovaltsov, 2011). Indeed, cosmogenic isotopes generated in the atmosphere by GCRs and stored in dateable terrestrial reservoirs such as ice sheets and tree trunks, are our only source of information on solar variability on millennial timescales (Beer, Vonmoos, and Muscheler, 2006). For the present study, GCR flux is inferred using high-latitude ground-based neutron monitors. As GCRs enter the terrestrial atmosphere, they collide with atmospheric particles, producing secondary particles such as neutrons, which are then observed at the detectors situated around the globe. The neutron monitor used for this study is at McMurdo, Antarctica, is run by the Bartol Institute, and has been recording data since 1964. The cut-off rigidity for this neutron monitor, set by the geomagnetic field, is lower than that set by the atmosphere because of the strength and more strongly vertical orientation in polar regions of the geomagnetic field. This means that the instrument responds to energies down to about 1 GeV, whereas a station near the Equator (where the cut-off rigidity is set by the geomagnetic field) will respond to particles of energy exceeding about 16 GeV. The fractional modulation of cosmic rays by the heliosphere is greater at lower energies, and hence by selecting this high-latitude station we detect the stronger variation of the lower-energy particles (Bieber *et al.*, 2004).

Schwabe (1843) was the first to recognise the 11-year solar-cycle variation using the periodicity in sunspot number records, and the signature of this variation in cosmic rays was detected using ionisation chambers by Forbush (1954). Evidence for the 22-year Solar Cycle variation was first reported on by Ellis (1899), who observed high counts of geomagnetically quiet days during alternate minima in the 1850s and 1870s. Chernosky (1966) showed additional characteristic differences in geomagnetic activity in alternate 11-year cycles. The odd- and even-numbered solar cycles have been shown to be different in cosmic ray fluxes at Earth (*e.g.* Webber and Lockwood, 1988), giving a 22-year cycle, known as the Hale Cycle, as also seen in sunspot polarity and latitude (Hale and Nicholson, 1925). Van Allen (2000) compared neutron counts with sunspot numbers for solar activity Cycles 19 – 22. He produced modulation cycles where each year a data point is plotted, between sunspot number and neutron counts, which map out an approximately circular pattern throughout the cycle. He showed that the shape of these plots was vastly different between the odd Solar Cycles 21 and 23 and the even Cycles 20 and 22. He also noted that as sunspot numbers increase after solar minimum, the cosmic ray flux drops quicker for odd than for even cycles.

Studies of the 22-year cycle in cosmic-ray fluxes from modern neutron monitors (*e.g.* Webber and Lockwood, 1988; Smith, 1990) have led to the description of neutron counts following an alternate flat-topped and peaked pattern. The polarity of the solar field $[A]$ is taken to be negative when the dominant polar field is inward in the northern and outward in the southern hemisphere (*e.g.* Ahluwalia and Ygbuhay, 2010; and references therein) and positive if the opposite is true. Curvature and gradient drift directions are reversed if the sign of the charge of the particle $[q]$ is reversed, therefore it is customary to define cycles by the polarity of the product $[qA]$. The occurrence of flat-topped and peaked maxima has been found to agree with the expected effect of curvature and gradient drifts of cosmic ray protons (Jokipii, Levy, and Hubbard, 1977; Jokipii and Thomas, 1981; Potgieter, 1995; Ferreira and Potgeiter, 2004): during cycles with positive polarity ($qA > 0$), cosmic ray protons arrive at Earth after approaching the poles of the Sun in the inner heliosphere and moving out

along the heliospheric current sheet (HCS). Conversely, during negative polarities ($qA < 0$), cosmic ray protons approach the Sun along the HCS plane and leave via the poles. The ease with which cosmic rays can travel toward Earth along the HCS during $qA < 0$ cycles is thought to depend on the HCS tilt (or inclination) relative to the solar Equator. Shielding of GCRs is also provided by scattering of particles off irregularities in the heliospheric field. Because the number and size of these irregularities tends to scale with the field strength, this is well quantified by the open solar flux (OSF) (Rouillard and Lockwood, 2004), the total magnetic flux leaving the coronal source surface (usually defined to be at a heliocentric distance of 2.5 $R_\odot$ where $R_\odot$ is a mean solar radius). Surveys of *in-situ* data show that the near-Earth interplanetary medium also displays 22-year cycles (*e.g.* Hapgood *et al.*, 1991), and the results of Rouillard and Lockwood (2004) suggest that the 22-year variation was primarily caused by that in heliospheric field strength, with less influence of drift effects than previously thought.

The polar-field reversal, which must separate $qA > 0$ and $qA < 0$ cycles, occurs at, or just after, sunspot maximum for each solar cycle. It is triggered by magnetic flux migrating up from sunspot groups towards the poles, which cancels out the pre-existing flux of opposite polarity already situated here (Harvey, 1996). This behaviour is clearly visible in photospheric magnetogram data.

The tilt angle of the heliospheric current sheet (HCS) has been shown to be a key parameter in the modulation of cosmic rays. The model proposed by Alanko-Huotari *et al.* (2007) suggested that the modulation can be described by a combination of the HCS tilt angle, the Sun's polarity, and the unsigned open solar flux (OSF). This model gives good agreement throughout Solar Cycles 19 – 23. Cliver and Ling (2001) compared the heliospheric tilt angle for Solar Cycle 21, 22, and the available data of Solar Cycle 23 at the time. They noted that during the declining phase of solar cycle, the decay of the HCS tilt angle following the odd cycle was more gradual than following the even cycle. During the ascending phase, however, both cycles were remarkably similar. From this, the authors concluded that this is most likely due to differences in the evolution of the large-scale magnetic field on the decay of the solar cycle. This study was updated by Cliver, Richardson, and Ling (2011), who added the HCS tilt-angle data for the remainder of Solar Cycle 23. They found that the recent cycle was indeed similar to Cycle 21 in shape, but that Solar Cycle 23 was much longer. In this article, we build on the studies of Cliver and Ling (2001) and Cliver, Richardson, and Ling (2011) by evaluating other heliospheric parameters to investigate the possible difference in the declining phase of the solar cycle, in particular, whether the difference between GCR flux in $qA < 0$ and $qA > 0$ cycles has its origin in differences in the heliospheric field strength and not just in its direction (as would be expected for drift effects alone).

2. The 22-Year Solar Cycle Variations

In this study, we consider "polarity cycles" to be the intervals between polar polarity reversals (*i.e.* solar maximum to solar maximum) and not the conventional solar cycle (*i.e.* from solar minimum to solar minimum), as has previously been studied. This enables us to better isolate effects of solar polarity. Thus, we assign a phase [ϵ_p], varying linearly between 0° and 360°, between the two polarity reversals (such that its relationship to the sunspot cycle phase [ϵ] defined from solar minimum to minimum by Lockwood *et al.* (2012) is $\epsilon_p \approx \epsilon - 2\pi x(4.5/L)$, where L is the solar-cycle length in years). However, polarity reversals are difficult to define from photospheric magnetogram data, as there are annual fluctuations in observed polar polarities due to the inclination of the ecliptic plane with respect to

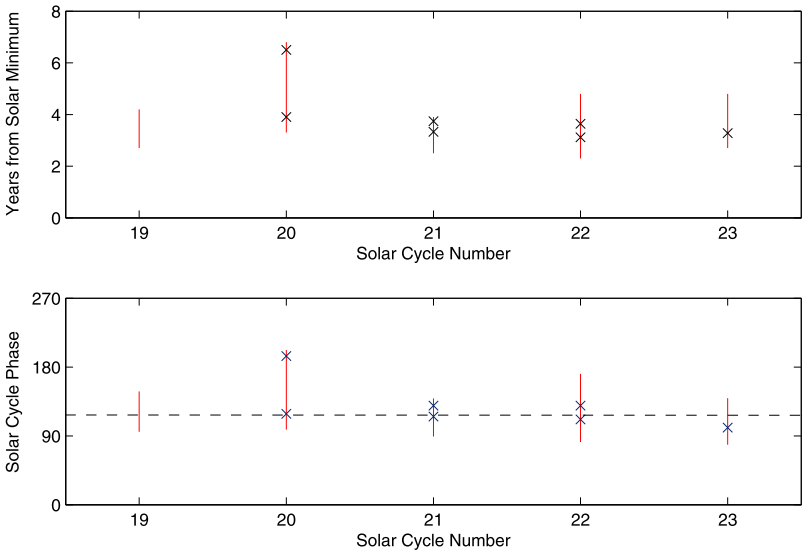

Figure 1 Solar polarity reversal times for Solar Cycles 19 to 23, as estimated from photospheric magnetograms. The red lines show the earliest and latest times that the average field of either the north or the south magnetic polar region crosses zero. Black crosses give best estimates for polarity reversals. The top panel shows the times from sunspot minimum in years, while the bottom panel shows solar-cycle phase [ϵ]. The dashed horizontal line in the bottom panel shows the value used here to determine the timing of polarity reversals from sunspot data.

the heliographic equator (Babcock and Babcock, 1955). Furthermore, polarity reversals do not occur simultaneously at both poles but are often separated by more than a year (Babcock, 1959). The present study used polarity reversal times for Solar Cycles 21 – 23 from Svalgaard, Cliver, and Kamide (2005) and Hathaway (2012), an extension to the polarity reversal of Solar Cycle 24 (see Lockwood *et al.*, 2012), and analysis from Babcock (1959) for Solar Cycle 20.

Within one solar hemisphere, the mean of the earliest and latest times at which the polarity reversal may have occurred, are defined as the times at which the average field in that polar region crosses zero. These are displayed in Figure 1 as the vertical red lines. The top panel shows these data in years since solar minimum, defined as the time of rapid increase in the average sunspot latitude (Owens *et al.*, 2011). The bottom panel shows the same polarity reversal data as a function of solar-cycle phase [ϵ], defined as 0° at the start of the solar cycle and 360° at the end of the solar cycle, which effectively normalises for the variable length of solar cycles. The black crosses in Figure 1 are the times when the average north minus average south polar fields cross zero. These data, however, are unavailable prior to Cycle 20 and so these crosses are not included in Figure 1. This is generally used as a measure of the global solar dipole having reversed (*e.g.* Hathaway, 2012).

To apply this analysis to pre-space-age solar cycles, it is necessary estimate the time of polarity reversals without the aid of photospheric magnetograms instead of relying only on sunspot data. We therefore calculated the solar cycle phase [ϵ] which is the best fit through all the potential times of polarity reversal shown in Figure 1. We found a phase of $\epsilon = 125°$, as shown by the horizontal dashed line, and this ϵ was used to define $\epsilon_p = 0°$. The error on the phase is 20° corresponding to an average of 0.5 to 1 year in the top panel. The blue ($qA > 0$) and red ($qA < 0$) lines in Figure 2 are based on polarity-reversal timings approximated

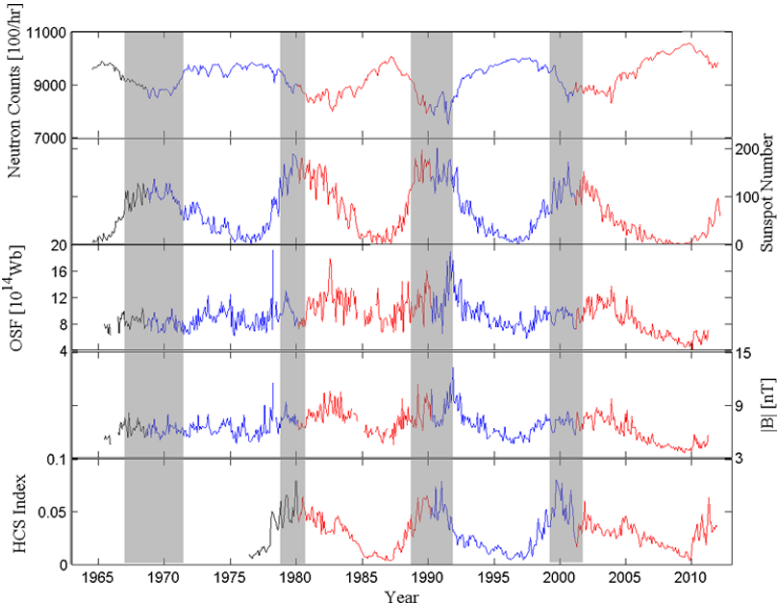

Figure 2 Time series (from top): neutron-monitor counts at McMurdo, sunspot number, unsigned open solar flux, magnitude of the heliospheric magnetic field in near-Earth space, and heliospheric current sheet tilt index. The 22-year solar cycle is clearly seen in the cosmic-ray count rates. The times of $qA < 0$ polarity are shown in red and $qA > 0$ in blue with the change in colours representing the polarity reversal time estimated using sunspot data. The grey boxes represent the times of polarity reversals estimated from photospheric magnetograms as described in the text.

by this method. The grey-shaded regions are the full extents of the polarity reversal times estimated from photospheric magnetograms. In general, the two methods agree well. This is because while solar cycle length can vary considerably; it tends to be a result of short or long declining phases, with rise phases showing much less variability in length (Waldmeier, 1935; Hathaway, Wilson, and Reichmann, 1994; Owens *et al.*, 2011).

The top panel of Figure 2 shows neutron monitor counts at McMurdo. The 22-year cycle in cosmic ray flux is clearly visible with its alternate flat-topped (blue) and peaked (red) pattern. The second panel shows the sunspot number. The third panel shows the unsigned open solar flux (OSF), calculated from $4\pi\,\mathrm{AU}^2|B_\mathrm{R}|$, where AU is the Earth–Sun distance and B_R is the daily mean radial magnetic field from the OMNI dataset (King and Papitashvili, 2005). The bottom panel shows the HCS index, a useful parameter for quantifying any tilt and the warped nature of the HCS (in other studies often called tilt angle). It is found by applying a uniform grid across the magnetogram-constrained potential-field source surface (PFSS) and computing the fraction of grid boxes that have the opposite polarity to their immediate longitudinal neighbour (Owens, Crooker, and Lockwood, 2011). At solar maximum, much of the HCS is highly inclined with the rotation axis, and it is highly warped due to a strong quadrupole moment, giving a high HCS index value. At solar minimum, when the quadrupole moment is weaker and the dipole more rotationally aligned, the HCS index has a much lower value. As discussed above, the HCS has been found to play a key role in the modulation of cosmic rays (*e.g.* Smith and Thomas, 1986) because distortions in the HCS are associated with corotating interaction regions (CIRs), which can act as shields to GCR propagation (Rouillard and Lockwood, 2007). Structures in the heliospheric mag-

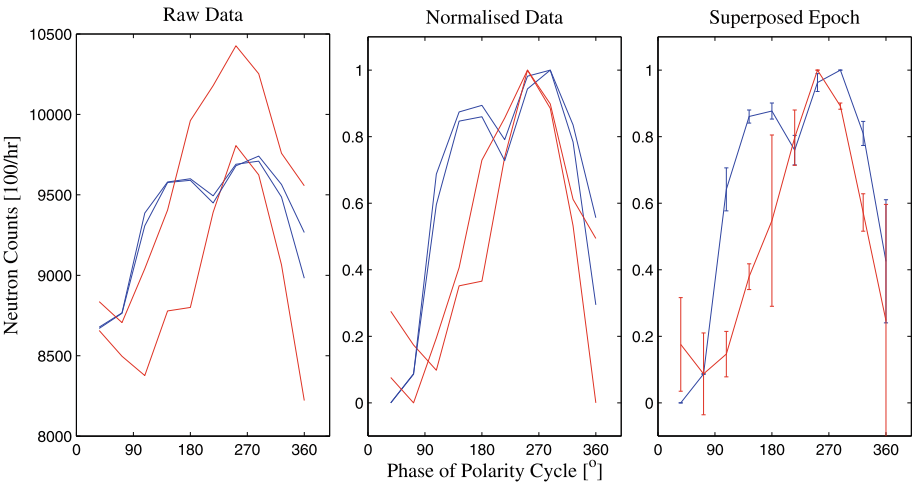

Figure 3 Neutron monitor counts as a function of polarity-cycle phase [ϵ_p] for $qA > 0$ (blue) and $qA < 0$ (red) cycles. From left: raw data, normalised data, and superposed epoch (composite) analysis. The error bars are plus or minus one standard deviation.

netic field can result in GCRs experiencing drift effects or scattering off of irregularities (*e.g.* Parker, 1965; Jokipii, Levy, and Hubbard, 1977). OSF is also included in a model by Alanko-Huotari *et al.* (2007), who found it to be strongly anti-correlated with neutron count rates (*e.g.* Lockwood, 2003; Rouillard and Lockwood, 2004). Note that the HCS inclination-index data show a more gradual decline during the declining phase of $qA < 0$ cycles than the $qA > 0$ cycles, as noted by Cliver and Ling (2001) and Cliver, Richardson, and Ling (2011).

3. Differences Between $qA < 0$ and $qA > 0$ Cycles

To examine the differences between heliospheric and GCR properties in $qA < 0$ and $qA > 0$ polarity cycles, we here used a superposed epoch (composite) analysis. To demonstrate the analysis process, we first applied this analysis to the neutron-monitor count rates in Figure 3.

The red lines in Figure 3 represent $qA < 0$ cycles while the blue lines are $qA > 0$ cycles. The left panel shows the raw data (27-day means) of the McMurdo neutron monitor count rates as a function of the polarity phase [ϵ_p] (defined using the sunspot method of defining the polarity-cycle start/end times). For the anticipitated polarity reversal of Cycle 24, we used the date of 2.4 months into 2013, corresponding to a phase of 125° through the polarity cycle (Lockwood *et al.*, 2012). The middle panel shows the data normalised to the maximum and minimum values over that individual polarity cycle to remove systematic cycle-to-cycle amplitude variations. Finally, the right panel shows the average for normalised parameters over $qA > 0$ and $qA < 0$ cycles, with error bars showing plus/minus one standard deviation.

The neutron-monitor count rates clearly show the Hale cycle. The $qA < 0$ and $qA > 0$ cycles display differing shapes, with the peaked and flat-top profiles largely the result of differences in the first half of the polarity cycle (*i.e.* the declining phase of the sunspot cycle), although there is a shorter, less pronounced difference after the cosmic ray peak (*i.e.* the rising phase of the sunspot cycle). In Figure 4 we now repeat this analysis for a number of other solar and heliospheric parameters.

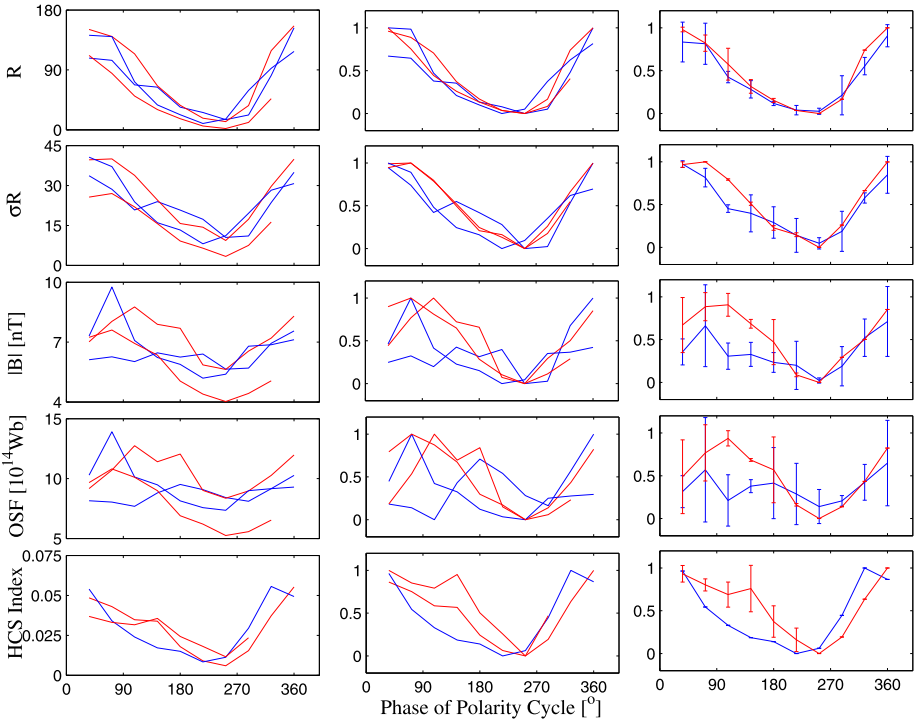

Figure 4 Panels from left to right give raw data, normalised data, and averages of the $qA < 0$ and $qA > 0$ polarity cycles (in red and blue, respectively). These plots are for (from top to bottom) the monthly sunspot number $[R]$, the monthly standard deviation of the daily sunspot number $[\sigma_R]$, the near-Earth magnetic-field strength $[|B|]$, the open solar flux [OSF], and the HCS inclination index. The error bars are plus and minus one standard deviation of the two polarity cycles used. Note that there are data on the HCS inclination index for only one $qA > 0$ cycle, therefore no standard deviations can be given in the bottom right panel. The data have been averaged over bins in cycle phase $[\epsilon_p]$ that are 36° wide.

The format of Figure 4 is the same as that for Figure 3, with raw data in the left column, normalised data in the middle, and a superposed epoch analysis shown on the right. The four rows show (from top to bottom) the international sunspot number $[R]$, the monthly standard deviation of daily sunspot number $[\sigma_R]$, the near-Earth magnetic-field strength $[|B|]$, the open solar flux [OSF], and the HCS inclination index. For the HCS inclination index, there is only one cycle of data available for $qA > 0$, therefore no error bars can be given.

The sunspot number shows a small difference between the $qA < 0$ and $qA > 0$ cycles, suggesting that the start and end times for the cycles are well defined and that there is no Hale effect in sunspot number $[R]$. However, the standard deviation of the sunspot number does show a significant difference between the two polarities: in the second panel, we see a greater variability in sunspot number during the $qA < 0$ polarity cycles than during the $qA > 0$ cycles. The increased variability could be the result of active longitudes (*e.g.* Ruzmaikin *et al.*, 2000; Berdyugina and Usoskin, 2003) separated by quiet longitudes. This agrees with an anti-correlation between cosmic ray flux and non-asymmetric open solar flux (Wang, Sheeley, and Rouillard, 2006), which is responsible for the longitudinal structure in the heliosphere. It is worth noting that Gil and Alanis (2008) found that the 27-day variability of neutron monitor counts was greater in $qA > 0$ cycles than in $qA < 0$ cycles. However,

this behaviour is opposite to that for the sunspot numbers noted here. This could be a result of rotating compression regions associated with the HCS known as corotating interaction regions (CIRs), which are more effective modulators during $qA > 0$ cycles (Richardson, Cane, and Wibberenz, 1999), and not the result of a change in CIR and/or heliospheric properties themselves.

A similar signature is also seen in the other three rows, which show the heliospheric magnetic field, the OSF, and the HCS inclination index. There is a significant difference between the $qA < 0$ and $qA > 0$ cycles around $\epsilon_{\rm p} = 125°$ (which corresponds to the declining phase of the solar cycle). The HCS inclination index result is also consistent with a greater prevalence of active longitudes during the declining phase of the solar cycle under $qA < 0$ conditions. A very similar pattern is also noted for the HCS tilt angle (not presented here). The only available $qA > 0$ cycle is consistently outside of the error bars throughout the first half of the polarity cycle, the time when the $qA < 0$ and $qA > 0$ cosmic ray values differ most significantly. Hence, the result for Cycle 23 is consistent with the previous findings of Cliver and Ling (2001).

Solar Cycle 20 was unusual in terms of the magnitude of the near-Earth magnetic field and because the OSF was particularly flat and showed little solar cycle variation. As can be seen from Figure 4, this cycle does indeed have an effect on the difference between the average behaviour of $|B|$ and the OSF within the $qA > 0$ and $qA < 0$ cycles. However, we note that removing this cycle does not remove the significance in the difference between average $qA > 0$ and $qA < 0$ cycles.

We also tested the sensitivity to changing the exact start and end times of the polarity cycles. Varying the boundaries between the times of the north and south polar reversals by an interval of 0.5 – 1 year (from the error on the phase in Figure 1) during the space age does vary the average curves to some degree. However, it does not remove the differences between the $qA > 0$ and $qA < 0$ cycles during the first half of the polarity cycle, which remains significant. This test is applied again and discussed in more detail in the next section.

4. Geomagnetic Reconstructions of the Pre-Space-Age Heliosphere

We now consider data from before the space age. Magnetic-field magnitude and OSF can be reliably reconstructed back to at least 1905 using geomagnetic data (*e.g.* Lockwood, Rouillard, and Finch, 2009; Lockwood and Owens, 2011). We used these data sets to examine the behaviour of the heliospheric magnetic field over six additional pre-space-age polarity cycles. This enabled us to test whether this difference in heliospheric parameters during the $qA > 0$ and $qA < 0$ polarity cycles is limited to the space-age, which spans the recent grand solar maximum (Solanki *et al.*, 2004; Lockwood, Rouillard, and Finch, 2009; Lockwood *et al.*, 2012), or whether it is a more persistent feature. Geomagnetic reconstruction of the heliospheric field is limited to yearly values because annual variations in factors such as the ionospheric conductivity and Earth's dipole tilt influence the coupling between the solar wind and the geomagnetic field. Thus bin sizes were taken to be approximately one year (precisely one year is not possible because we consider solar cycle phase, not time). Between the geomagnetic reconstructions and the OMNI data, heliospheric magnetic field magnitude and open solar flux have been shown to be consistent (Lockwood and Owens, 2011). We therefore assumed that these parameters agree during the space-age and that geomagnetic reconstructions can be taken as representative of the heliospheric magnetic field throughout the period of 1905 – 2012.

Figures 5 and 6 give a similar analysis to Figure 4 in the same format as Figures 3 and 4, namely for the raw data (left column), normalised data (middle column), and means and

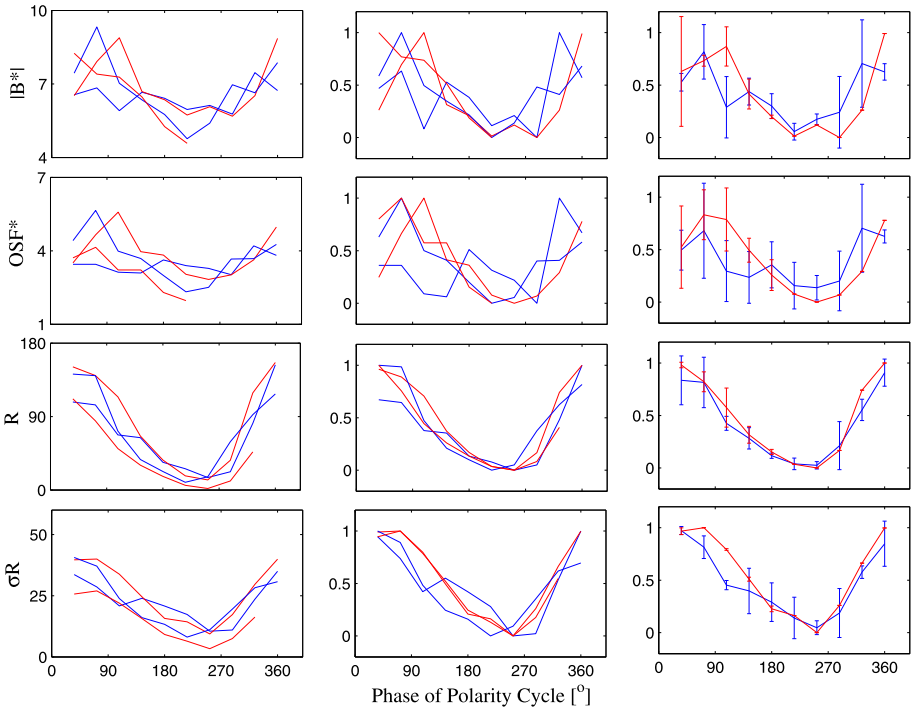

Figure 5 Heliospheric magnetic-field magnitude [$|B^*|$] and open solar flux [OSF*] reconstructed from geomagnetic data, along with the monthly sunspot number and the monthly standard deviation of the daily sunspot number. This plot considers the space-age period (1965 – 2012). The red curves show $qA < 0$ polarity cycles for each parameter, whereas the blue curves show $qA > 0$ cycles. The left column shows the raw data, the middle column shows the data normalised to the maximum and minimum values, and the right column gives the mean and standard deviations of the polarity cycles.

standard deviations (right column) of the $qA < 0$ and $qA > 0$ polarity cycles (in blue and red, respectively) determined using the sunspot method of defining ϵ_p. This analysis is given for (from top) $|B^*|$ the heliospheric magnetic-field magnitude, and OSF* the open solar flux (where the asterisks denote that values are reconstructed from geomagnetic data), along with monthly sunspot numbers and the monthly standard deviation of the daily sunspot number.

Figure 5 shows the space-age data only, whereas Figure 6 gives the pre-space-age data. As can be seen from Figure 5, the difference between the $qA < 0$ and $qA > 0$ cycles during the space age is still present in $|B^*|$ and OSF*. Because the reconstructed data have a yearly resolution, the data are binned more coarsely, with fewer data points averaged to produce each data point, which may partly explain why the differences in $|B^*|$ and OSF* are slightly less pronounced than for $|B|$ and OSF in Figure 4. The sunspot numbers and standard deviations are also plotted at this yearly resolution and show the same trends as found previously for the monthly averages. Note that the geomagnetic data do not cover the final 72° of the polarity-cycle phase. This is because the geomagnetic data are only available up until June 2008, while in this study the main focus times are the declining phases of the solar cycle.

Figure 6 shows the same analysis as Figure 5, but for six pre-space-age polarity cycles. The pre-space-age $|B^*|$ and OSF* do show some slight differences in alternate polarity cycles; however, unlike the space age, these are earlier in the polarity cycle (*i.e.* just after

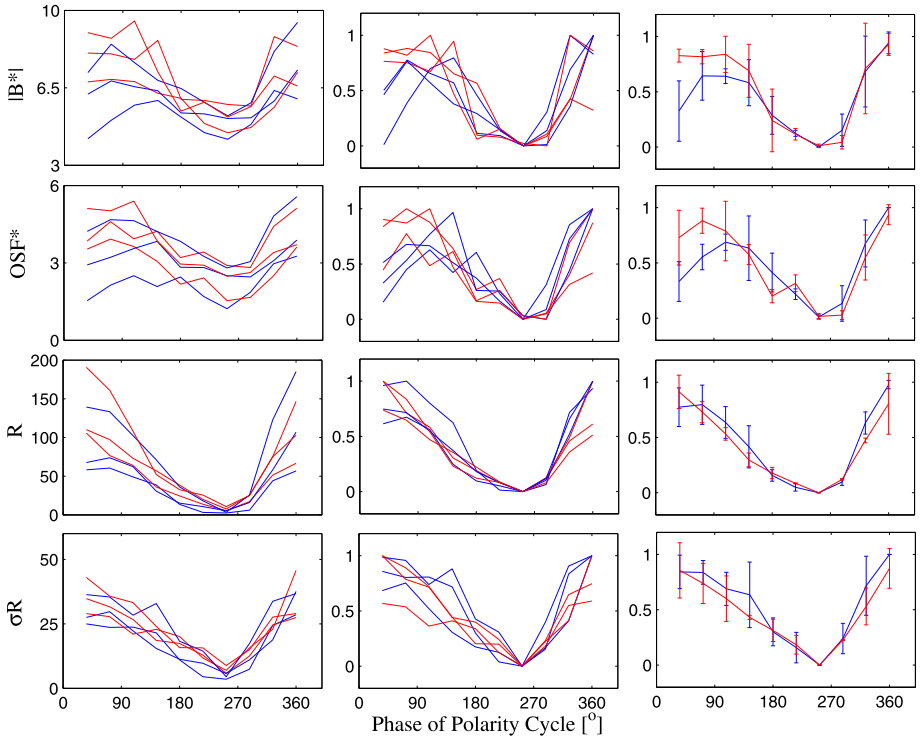

Figure 6 Pre-space-age reconstructions of heliospheric magnetic-field magnitude [$|B^*|$] and open solar flux [OSF*]; the sunspot number and standard deviation of daily sunspot number are also shown. The red curves show $qA < 0$ polarity cycles for each parameter, whereas the blue curves show $qA > 0$ cycles. The left column shows the raw data, the middle column shows the normalised data, and the right column is a superposed epoch analysis.

solar maximum) and hence no longer coincident with the Hale Cycle differences in the cosmic-ray flux. Furthermore, the standard deviation of daily sunspot numbers with respect to the monthly averages does not show the same variation between alternate polarity cycles in the pre-space-age data (in fact, the $qA > 0$ cycles give slightly higher mean values at the relevant ϵ_p than the $qA < 0$ cycles in Figure 5, but the difference is small compared to the errors).

We now test the sensitivity of the results shown in Figures 5 and 6 to realistic variations on the start and end times of the polarity cycle (*i.e.* changes in the time of polarity reversal). Comparison of the polarity-reversal times determined from sunspot number and photospheric magnetograph data (Figure 1) suggests a typical uncertainty of around 0.5 years. Therefore we performed a Monte Carlo analysis of the difference in heliospheric parameters in the $qA < 0$ and $qA > 0$ cycles to the varying the reversal times by half a year. For each variable shown in Figures 5 and 6 (*i.e.* the geomagnetic reconstructions of magnetic-field magnitude and OSF, the monthly sunspot number, and the sunspot variance) we used random numbers to vary the start and end times of each cycle by 0.5 years with a chosen weighting of 50 % chance of no change in start and end time and 50 % of the reversal time changing by 0.5 years (with an equal probability of moving backward or forward 0.5 years). For each set of new polarity reversal times, we repeated the same superposed-epoch analy-

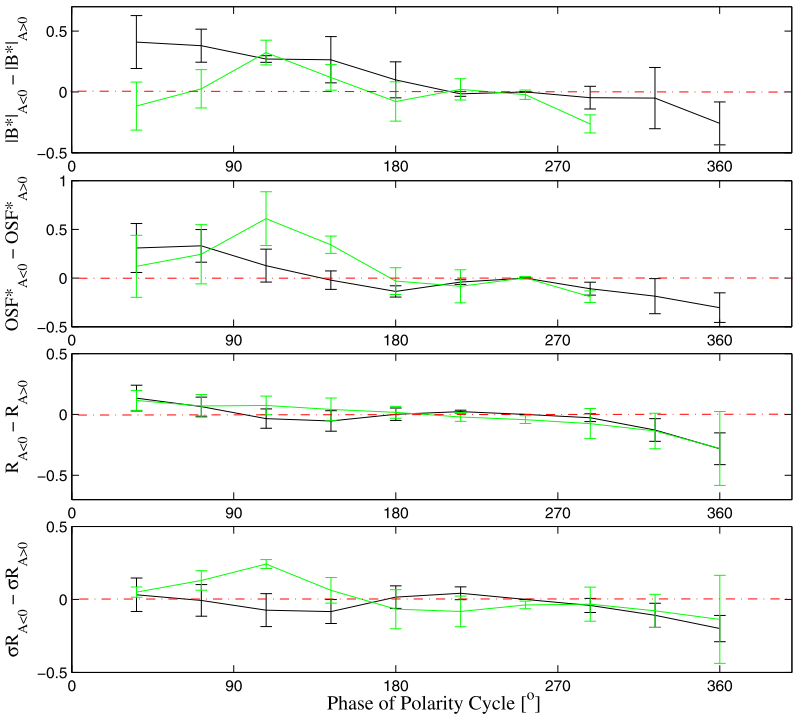

Figure 7 Sensitivity analysis of geomagnetic and sunspot data to varying the start and end dates by plus or minus 0.5 years. Each panel shows the difference between $qA < 0$ and $qA > 0$ polarity cycles of the following parameters (from top): reconstructed magnetic-field intensity, reconstructed open solar flux, sunspot number, and sunspot variance. The green line shows the mean of all space-age cycles and the black line shows all pre-space-age cycles with the error bars representing the standard deviation of all cycles included in the mean.

sis and computed the difference in the $qA > 0$ and $qA < 0$ parameters. We ran this process 1 000 times to obtain a broad spread of cycle start and end times.

Figure 7 shows the difference in heliospheric parameters between the $qA > 0$ and $qA < 0$ cycles, with the space age (pre-space age) in green (black). Shown from top to bottom are geomagnetic reconstructions of the heliospheric magnetic field $[|B^*|]$, the open solar flux $[\mathrm{OSF}^*]$, the sunspot number $[R]$, and the sunspot variance $[\sigma_\mathrm{R}]$, as used in previous plots. Each parameter was averaged over all available cycles of each polarity and the differences between the means for the $qA < 0$ and $qA > 0$ cycles are plotted. The green lines are the average behaviour of all space-age cycles and the black lines are all pre-space-age cycles. The error bars on each plot are plus or minus the standard deviation of all cycles included in the mean of all samples.

For the heliospheric magnetic-field strength $[|B^*|]$ (top panel) both the pre-space-age data (black line) and the space-age data (green line) show a difference around $\epsilon_\mathrm{p} = 100°$, which is larger than the error bars and so is considered significant. This difference is significant at all phases of the declining phase of the sunspot cycle ($\epsilon_\mathrm{p} < 100°$) for the pre-space-age data, but not for shortly after solar maximum in the space-age data. This means that shortly after sunspot maximum, $|B^*|$ during $qA < 0$ cycles is larger than for $qA > 0$ cycles in the pre-space-age data, which is the opposite of the space-age data. The result that there

is no significant difference between the two polarity cycles for sunspot number [R] is found not to be sensitive to the start and end times of cycles used.

On the other hand, for both the OSF* and the sunspot number variability [σ_R], the result holds when subjected to sensitivity testing; that is, the declining phases of the space-age cycles show an increase in these parameters during $qA < 0$ over $qA > 0$, but do not show a difference in pre-space-age data. This is shown as the peak in the space-age data above the pre-space age is more than zero by more than the error bar.

Another result to note is the difference at the start of the polarity cycle seen in the geomagnetic $|B^*|$ data. Here we see $|B^*|$ during $qA < 0$ dominating $|B^*|$ during $qA > 0$ during pre-space-age cycles, but the opposite is true for space-age cycles. This result may warrant further work but is not seen in any other variable.

5. Discussion and Conclusions

As cosmic rays are modulated by the heliospheric magnetic field and heliospheric current-sheet tilt, the 11-year cycle is also seen in cosmic ray records. In addition to the solar cycle, cosmic ray time series display a strong 22-year Hale Cycle, which has been attributed to differing drift patterns and diffusion (particularly at solar maximum) during positive and negative solar field polarities (*e.g.* Jokipii, Levy, and Hubbard, 1977; Ferreira and Potgeiter, 2004). It has been argued that this results in the earlier rise to the cosmic ray peak during $qA > 0$ cycles than for $qA < 0$ cycles, and gives the time series a flat-topped and peaked appearance, respectively. However, an increasing number of results are not consistent with this concept. For example, Richardson, Cane, and Wibberenz (1999) and Gil and Alanis (2008) have found that recurring decreases in cosmic ray fluxes were considerably stronger when $qA > 0$, whereas the drift theory suggests that they should be stronger for $qA < 0$, when cosmic rays should be entering by drifting inward along the HCS. In addition, other studies have found differences between $qA > 0$ and $qA < 0$ in the HCS tilt (Cliver and Ling, 2001) and in open solar flux (Rouillard and Lockwood, 2004) that offer alternative explanations of the 22-year cycle in cosmic ray fluxes.

In this study, we separated space-age solar and heliospheric data into polarity cycles defined as intervals between polar solar-polarity reversals, thus approximately spanning solar maximum to solar maximum.

The results show a significant difference in the behaviour of HCS inclination, heliospheric magnetic-field magnitude, and open solar flux between $qA > 0$ cycles and $qA < 0$ cycles. This difference is only significant during the first half of the polarity cycle, which corresponds to the declining phase of the solar cycle, the period responsible for a large part of the difference in GCR fluxes in the $qA > 0$ and $qA < 0$ cycles. The standard deviation in daily sunspot number also gives a significant difference between $qA > 0$ and $qA < 0$ cycles during the same period, suggesting a greater prevalence of active longitudes during this phase of $qA < 0$ cycles. This agrees with the increased HCS inclination throughout this period. The presence of more active longitudes giving greater HCS inclination means that there will be regular fast/slow stream interfaces extending over broad latitudinal ranges, which was shown to be an effective way of shielding cosmic rays in a case study by Rouillard and Lockwood (2007).

We suggest that the 22-year cycle in GCR flux may be partly due to direct heliospheric modulation, although drift effects (Jokipii, Levy, and Hubbard, 1977; Ferreira and Potgeiter, 2004) will still play a role, particularly during the end of the polarity cycle (*i.e.* the rise phase of the solar cycle), when differences in heliospheric parameters are less apparent. Of course,

while changes in heliospheric structure are coincident with the differing behaviour in cosmic ray flux in alternate polarity cycles, it still remains to be shown that they are of sufficient magnitude to effect the required modulation. To do this will, however, require a significant modelling effort.

The above conclusions relate to the space-age era for which there are *in-situ* observations of interplanetary parameters and magnetograph data from which the start and end times of the polarity cycle and the HCS tilt index can be derived. Because these data have been taken during a grand solar maximum (Lockwood, Rouillard, and Finch, 2009), the conclusions might not necessarily have been valid in the less active times prior to the grand maximum. To test this, the open solar flux and near-Earth magnetic field reconstructed from geomagnetic activity data were used, employing the sunspot number variations to define the start and end times of the polarity cycle. The data were divided into the space-age era (1965 and after corresponding to the first study) and pre-space-age data before 1965.

The reconstructed data from the space-age era supported the above findings of the study using direct observations, but we also noted that the differences between polarity cycles are considerably smaller before the space age. Using geomagnetic reconstructions of heliospheric magnetic-field magnitude and open solar flux, it was shown that for the period of 1905 – 1965, the opposite polarities do not give such differing patterns during the declining phase of the solar cycle. In particular, the variability in sunspot numbers is greatly reduced. One source of uncertainty that we addressed is that before the space age we have to use the sunspot number variation to define the start and end time of the polarity cycles. A sensitivity study that added the uncertainty in these inferred times showed that the result is robust for the open solar flux [OSF] and the variability of the sunspot number [σ_R]. However, this uncertainty means that we cannot be certain that the polarity effect on the near-Earth heliospheric field strength (at the phase of the polarity cycle when the polarity effect on GCR is greatest in the space-age era) is different in the pre-space-age data compared with the space-age era.

The data suggest that the polarity-dependent effect on cosmic rays before the recent grand solar maximum was most likely restricted to the drift effects and was not as marked as it has been in recent data. This is consistent with cosmogenic isotope data, which, in general, do not show strong 22-year Hale cycle variations (Usoskin, 2008).

Acknowledgements We are grateful to the Space Physics Data Facility (SPDF) of NASA's Goddard Space Flight Centre for combining the data into the OMNI 2 data set, which was obtained via the GSFC/SPDF OMNIWeb interface at omniweb.gsfc.nasa.gov and to the Marshall Space Flight Centre for the Sunspot Number data obtained from MSFC at solarscience.msfc.nasa.gov/greenwch.shtml. We also thank the Bartol Research Institute of the University of Delaware for the neutron-monitor data from McMurdo, which is supported by NSF grant ATM-0527878 and J.T. Hoeksema of Stanford University for WSO magnetograms. The work of SRT is supported by a studentship from the UK's Natural Environment Research Council (NERC).

References

Ahluwalia, H.S., Ygbuhay, R.C.: 2010, *Status of Galactic Cosmic Ray Recovery from Sunspot Cycle 23 Modulation* **CP-1216**, AIP, New York, 699 – 702.

Alanko-Huotari, K., Usoskin, I.G., Mursala, K., Kovaltsov, G.A.: 2007, Cyclic variations of the heliospheric tilt angle and cosmic ray modulation. *Adv. Space Res.* **40**, 1064 – 1069.

Babcock, H.D.: 1959, The Sun's polar magnetic field. *Astrophys. J.* **130**, 364 – 366. ADS:1959ApJ...130..364B, doi:10.1086/146726.

Babcock, H.W., Babcock, H.D.: 1955, The Sun's magnetic field 1952 – 1954. *Astrophys. J.* **121**, 349.

Beer, J., Vonmoos, M., Muscheler, R.: 2006, Solar variability over the past several millennia. *Space Sci. Rev.* **125**, 67 – 79.

Berdyugina, S.V., Usoskin, I.G.: 2003, Active longitudes in sunspot activity: century scale persistence. *Astron. Astrophys.* **405**, 1121 – 1128.
Bieber, J.W., Clem, J.M., Duldig, M.L., Evenson, P.A., Humble, J.E., Pyle, R.: 2004, Latitudinal survey observations of neutron monitor multiplicity. *J. Geophys. Res.* **109**. doi:10.1029/2004JA010493.
Chernosky, E.J.: 1966, Double sunspot-cycle variation in terrestrial magnetic activity. *J. Geophys. Res.* **71**, 965.
Cliver, E.W., Ling, A.G.: 2001, 22 year patterns in the relationship of sunspot number and tilt angle to cosmic-ray intensity. *Astrophys. J.* **551**, 189 – 192.
Cliver, E.W., Richardson, I.G., Ling, A.G.: 2011, Solar drivers of 11-year and long-term cosmic ray modulation. *Space Sci. Rev.* doi:10.1007/s11214-011-9746-3.
Ellis, W.: 1899, On the relation between magnetic disturbances and the period of solar spot frequency. *Mon. Not. Roy. Astron. Soc.* **60**, 142 – 157.
Ferreira, S.E.S., Potgeiter, M.S.: 2004, Long-term cosmic-ray modulation in the heliosphere. *Astrophys. J.* **603**, 744 – 752.
Forbush, S.E.: 1954, Worldwide cosmic ray variations, 1937 – 1952. *J. Geophys. Res.* **59**, 525 – 542.
Gil, A., Alanis, M.V.: 2008, On the energy spectrum of the 27-day variation of the galactic cosmic ray intensity. In: *Proc. 30th Internat. Cosmic Ray (ICRC07) Conf.* **1 (SH)**, 601 – 604.
Hale, G.E., Nicholson, S.B.: 1925, The law of Sun-spot polarity. *Astrophys. J.* **62**, 270 – 300.
Hapgood, M.A.: 2010, Towards a scientific understanding of the risk from extreme space weather. *Adv. Space Res.* **47**, 2059 – 2072.
Hapgood, M.A., Bowe, G., Lockwood, M., Willis, D.M., Tulunay, Y.: 1991, Variability of the interplanetary magnetic field at 1 A.U. over 24 years: 1963 – 1986. *Planet. Space Sci.* **39**, 411 – 423.
Harvey, K.L.: 1996, Large scale patterns of magnetic activity and the solar cycle. *Bull. Am. Astron. Soc.* **28**, 867.
Hathaway, D.H.: 2012, The solar cycle. *Living Rev. Solar Phys.* **7**, 1. doi:10.12942/lrsp-2010-1.
Hathaway, D.H., Wilson, R.M., Reichmann, E.J.: 1994, The shape of the sunspot cycle. *Solar Phys.* **151**, 177 – 190. ADS:1994SoPh..151..177H, doi:10.1007/BF00654090.
Jokipii, J.R., Thomas, B.: 1981, Effects of drift on the transport of cosmic rays IV. Modulation by a wavy interplanetary current sheet. *Astrophys. J.* **243**, 1115 – 1122.
Jokipii, J.R., Levy, E.H., Hubbard, W.B.: 1977, Effects of particle drift on cosmic-ray transport. I. General properties, application to solar modulation. *Astrophys. J.* **213**, 861 – 868.
King, J.H., Papitashvili, N.E.: 2005, Solar wind spatial scales in and comparisons of hourly wind and ACE plasma and magnetic field data. *J. Geophys. Res.* **110**. doi:10.1029/2004JA010649.
Lockwood, M.: 2003, Twenty-three cycles of changing open solar magnetic flux. *J. Geophys, Res.* **108**. doi:10.1029/2002JA009431.
Lockwood, M.: 2010, Solar change and climate: an update in the light of the current exceptional solar minimum. *Proc. Roy. Soc. A* **466**, 303 – 329.
Lockwood, M., Owens, M.J.: 2011, Centennial changes in the heliospheric magnetic field and open solar flux: the consensus view from geomagnetic data and cosmogenic isotopes and its implications. *J. Geophys, Res.* **116**. doi:10.1029/2010JA016220.
Lockwood, M., Rouillard, A.P., Finch, I.D.: 2009, The rise and fall of open solar flux during the current grand solar maximum. *Astrophys. J.* **700**, 937 – 944.
Lockwood, M., Owens, M.J., Barnard, L., Davis, C.J., Thomas, S.R.: 2012, What is the Sun up to? *Astron. Geophys.* **53**, 3.9 – 3.15.
McCracken, K.G., McDonald, F.B., Beer, J., Raisbeck, G., Yiou, F.: 2004, A phenomenological study of the long-term cosmic ray modulation, 850 – 1958 AD. *J. Geophys, Res.* **109**. doi:10.1029/2004JA010685.
Mewaldt, R., Davis, A., Lave, K., Leske, R., Stone, E., Wiedenbeck, M., Binns, W., Christian, E., Cummings, A., De Nolfo, G., Israel, M., Labrador, A., Von Rosenvinge, T.: 2010, Record-setting cosmic ray intensities in 2009 and 2010. *Astrophys. J. Lett.* **723**, L1 – L6.
Owens, M.J., Crooker, N.U., Lockwood, M.: 2011, How is open solar flux lost over the solar cycle? *J. Geophys. Res.* **116**. doi:10.1029/2011JA016039.
Owens, M.J., Lockwood, M., Barnard, L., Davis, C.J.: 2011, Solar cycle 24: implications for energetic particles and long-term space climate change. *Geophys. Res. Lett.* **38**, 19106.
Parker, E.N.: 1965, The passage of energetically charged particles through interplanetary space. *Planet. Space Sci.* **13**, 9 – 49.
Potgieter, M.S.: 1995, The time-dependent transport of cosmic rays in the heliosphere. *Astrophys. Space Sci.* **116**. doi:10.1029/2010JA016220.
Richardson, I.G., Cane, H.V., Wibberenz, G.: 1999, A 22-year dependence in the size of near-ecliptic corotating cosmic ray depressions during five solar minima. *J. Geophys. Res.* **104**, 12549.

Rouillard, A., Lockwood, M.: 2004, Oscillations in the open solar magnetic flux with a period of 1.68 years: imprint on galactic cosmic rays and implications for heliospheric shielding. *Ann. Geophys.* **22**, 4381 – 4395.

Rouillard, A., Lockwood, M.: 2007, The latitudinal effect of co-rotating interaction regions on galactic cosmic rays. *Solar Phys.* **245**, 191 – 206. ADS:2007SoPh..245..191R, doi:10.1007/s11207-007-9019-1.

Ruzmaikin, A.A., Feynman, J., Neugebauer, M., Smith, E.J.: 2000, On the nature and persistence of preferred longitudes of solar activity. *Bull. Am. Astron. Soc.* **32**, 835.

Schwabe, M.: 1843, Die Sonne. Von Herrn Hofrath Schwabe. *Astron. Nachr.* **20**, 283.

Smith, E.J.: 1990, The heliospheric current sheet and modulation of galactic cosmic rays. *J. Geophys. Res.* **95**, 18731 – 18743.

Smith, E.J., Thomas, E.J.: 1986, Latitudinal extent of the heliospheric current sheet and modulation of galactic cosmic rays. *J. Geophys. Res.* **91**, 2933 – 2942.

Solanki, S.K., Usoskin, I.G., Kromer, B., Schuessler, M., Beer, J.: 2004, Unusual acticity of the Sun during recent decades compared to the previous 11 000 years. *Nature* **431**, 1084 – 1087.

Svalgaard, L., Cliver, E.W., Kamide, Y.: 2005, Cycle 24: smallest in 100 years? *Geophys. Res. Lett.* **32**. doi:10.1029/2004GL021664.

Usoskin, I.G.: 2008, A history of solar activity over millennia. *Living Rev. Solar Phys.* **5**, 1 – 60. doi:10.12942/lrsp-2008-3.

Usoskin, I.G., Bazilevskaya, G.A., Kovaltsov, G.A.: 2011, Solar modulation parameter for cosmic rays since 1936 reconstructed from ground-based neutron monitors and Ionization chambers. *J. Geophys. Res.* **116**. doi:10.1029/2010JA016105.

Van Allen, J.A.: 2000, On the modulation of galactic cosmic ray intensity during solar activity cycles 19, 20, 21, 22 and early 23. *Geophys. Res. Lett.* **27**, 2453 – 2456.

Waldmeier, M.: 1935, Neue Eigenschaften der Sonnenfleckenkurve. *Astron. Mitt. Zurich* **14**, 105 – 130.

Wang, Y.M., Sheeley Jr., N.R., Rouillard, A.P.: 2006, Role of the Sun's nonaxisymmetric open flux in cosmic ray modulation. *Astrophys. J.* **644**, 638.

Webber, W.R., Lockwood, J.A.: 1988, Characteristics of the 22-year modulation of cosmic rays as seen by neutron monitors. *J. Geophys. Res.* **93**, 8735 – 8740.